The spectral dimension of aggregates of tunable fractal dimension

1995 J. Phys.: Condens. Matter 7 9703

(http://iopscience.iop.org/0953-8984/7/50/004)

J. Phys.: Condens. Matter 7 (1995) 9703–9714. Printed in the UK

The spectral dimension of aggregates of tunable fractal dimension

Romain Thouy†, Rémi Jullien† and Claude Benoit‡

† Laboratoire de Science des Matériaux Vitreux, UA 1119 CNRS Université Montpellier II, Place E Bataillon, CC 069, 34095 Montpellier Cédex 5, France

‡ Groupe de Dynamique des Phases Condensées, URA CNRS 233, Université Montpellier II, Place E Bataillon, CC 026, 34095 Montpellier Cédex 5, France

Received 16 June 1995, in final form 3 August 1995

Abstract. The dynamic properties of fractal aggregates with tunable fractal dimension are studied. The fractal dimensions are investigated in the range $1.0 \leqslant D \leqslant 2.5$. The interactions are represented by the Born scalar model and two kinds of rule describing links between particles are used. The spectral dimension is determined by computing the integrated density of states (IDOS), using the very fast spectral moments method. Comparisons with a direct diagonalization prove the efficiency of this method. Furthermore, we give a Brownian diffusion approach, which agrees with the moments method, for D lower than two. It is found that the spectral dimension strongly depends on the fractal dimension and, for fractal dimension larger than two, it varies with the degree of connectivity taken into account in the model.

1. Introduction

Over the past few years, fractal structures have been the subject of much attention. The most widely studied systems include aggregation phenomena. Several aggregation models have been proposed in order to describe fractal objects such as colloid and aerosol aggregates, clusters of balls floating on water [1], etc. We have already introduced an aggregation model which is able to build aggregates with fractal dimensions ranging from 1 up to 2.5, the *variable-D model* [2]. In this paper, we use this model to perform a systematic study of the dynamic properties as a function of the fractal dimension. The dynamical properties of fractal structures have been studied for a long time. The density of states on a fractal structure was studied for the first time by Alexander and Orbach in 1982 [3]; they took the scaling properties of the mass and the connectivity into account. From these investigations, it is known that the vibrational density of states varies as a power $(d_s - 1)$ of the frequency above a phonon-to-fracton crossover frequency ω_c, where d_s is the *spectral* dimension. Our aim is to calculate the spectral dimension on fractal structures with varying fractal dimension. Until now, most of the studies of fracton excitations [4] in fractal structures have been done using percolation networks, and a few deterministic fractal structures (like the Sierpinski gasket). In each case, the fractal dimension was fixed and could not be changed. Moreover it is known that percolation theory, which is restricted to equilibrium situations, cannot explain certain structures obtained via irreversible growth phenomena [1]. Therefore, since the density of states has been investigated by neutron scattering in real disordered systems (like aerogels), it would be interesting to be able to calculate it on the basis of different simulation models for these real materials. For that purpose, we use an

0953-8984/95/509703+12$19.50

aggregation model which builds aggregates of tunable fractal dimensions, and we employ a powerful tool to find their spectral density. The main principles of the variable-D model are reported in section 2. In section 3, we present the dynamic model used and a summary of the spectral moments method. The Brownian diffusion approach is developed in section 4, with the related theory. Global results for moments and diffusion methods are presented in section 5, followed by a discussion. A comparison with existing experiments on aerogels and a conclusion are given in section 6.

2. The variable-D model

The model uses a cluster–cluster hierarchical algorithm, on a d-dimensional hypercubic lattice with unit lattice parameter. We start the iterative growth from a collection of 2^n identical particles. We stick the particles, one by one, to obtain 2^{n-1} dimers (first iteration). At iteration p, we have a collection of 2^{n-p} aggregates, containing 2^p particles each. The growth stops when $p = n$, and we obtain a final aggregate of 2^n particles. So, to stick two aggregates of $N/2$ particles together, the distance Γ between their centres of mass should satisfy, in our model, the condition

$$\Gamma^2 = k^2 R_{N/2}^2 + 1 \tag{1}$$

where $R_{N/2}^2$ is the mean square radius of gyration of the two aggregates, and k is related to the desired fractal dimension D, by the relation

$$k^2 = 4(4^{1/D} - 1). \tag{2}$$

(*In practice, we try to minimize the absolute difference between the two sides of equation* (1) [2].) If several configurations satisfy relation (1), the final one is chosen at random among all the possibilities. In this work, we have considered version B of the model (using the terminology of [2]) in which some rotations of the clusters are allowed when trying to satisfy relation (1). The square of the radius of gyration has been averaged over the 2^{n-p} clusters of $N = 2^p$ particles obtained at each iteration. Then, instead of making a least-squares fit of the log–log plot of N versus $\sqrt{\langle R_N^2 \rangle}$, we have calculated an N-dependent fractal dimension $D(N)$ obtained by comparing the results from one iteration to the next one [5]:

$$D(N) = \frac{\log 4}{\log(\langle R_N^2 \rangle - \frac{1}{4}) - \log\langle R_{N/2}^2 \rangle}. \tag{3}$$

The term $\frac{1}{4}$ is introduced to eliminate 'trivial' corrections to scaling [5, 6]. In figure 1(a), we plot $D(N)$ versus $1/N$ for input $D = 1$, 1.5, 2, 2.5 and 3, in $d = 3$ [2]. As explained in [2], a fractal dimension longer than $\simeq$2.5 cannot be recovered with this model. In the following, we use the variable-D model to get aggregates with fractal dimension D ranging from 1.0 up to 2.5. In figure 1(b), we present a projection of three aggregates with $D = 1.5$, 2 and 2.5.

We need several samples for each fractal dimension to work out the averages. For the study of the spectral dimension, we consider two kinds of link rule, called:

(i) ALLINKS: links to all first neighbours are considered;

(ii) ONELINK: only the real links created by the aggregation model are considered; there are no loops, i.e. $N - 1$ links for an aggregate of N particles.

In figure 2, it can be seen how we stick two aggregates of four particles together (one is represented by open circles, and the other by filled circles), following ONELINK and

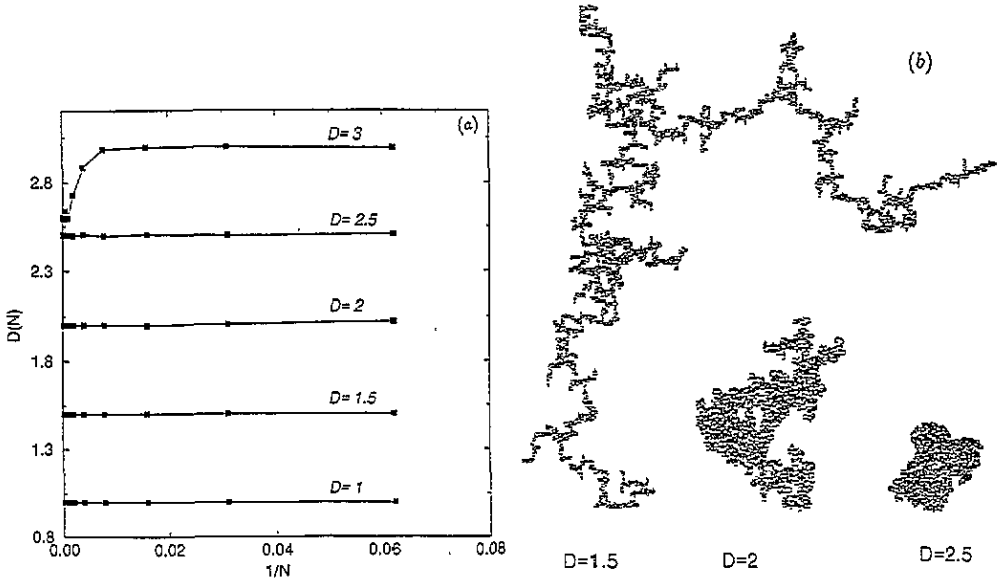

Figure 1. (*a*) Plot of $D(N)$ versus $1/N$, for $d = 3$, for $D = 1$, 1.5, 2, 2.5 and 3, from single runs up to 8192 particles (version B of [2]). (*b*) Projection of three aggregates ($N = 8192$ particles) with fractal dimensions $D = 1.5$, 2 and 2.5, on the same scale.

ALLINKS rules. We have drawn all aggregation bonds as bold springs. There is much interest in studying these two cases: the ONELINK case is very close to what would be obtained in a real cluster–cluster process with 'rigid' clusters, while the ALLINKS case would correspond to some degree of 'restructuring' when extra bonds can be formed (due to cluster flexibility or free rotation of bonds). Since some loops are created in the ALLINKS case (which are not present in the ONELINK case), it is interesting to know whether or not they are relevant in modifying the properties of the spectral density.

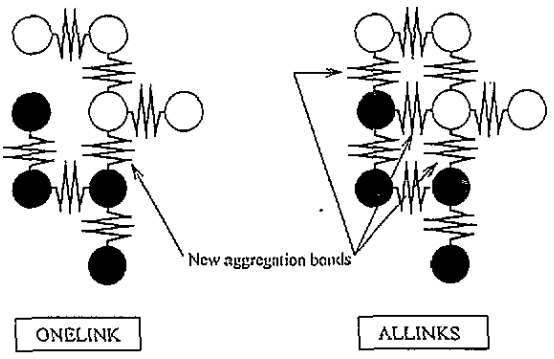

Figure 2. The final aggregate with eight particles ($d = 2$), obtained by sticking two aggregates of four particles each (open and filled circles) together, where bonds are represented by springs. In the case ALLINKS, there are nine bonds, in the case ONELINK, there are seven bonds.

3. The spectral moments method

3.1. The model

We now assume that the particles are connected by springs. The displacements of the particles are represented by scalars. Then, the set of equations of motion for the site i is given by

$$m\ddot{U}_i = -\sum_j \gamma_{ij} k U_j = -\sum_j k_{ij} U_j \tag{4}$$

with

$$k_{ij} = -\sum_{j \neq i} \gamma_{ij} k. \tag{5}$$

U_i is the scalar displacement of the site i, k_{ij} are the force constants between particles i and j, γ_{ij} are coefficients depending on the linkage rules. For the ALLINKS model, $\gamma_{ij} = 1$, if i and j are occupied, while with the ONELINK model, $\gamma_{ij} = 1$ only if a real link has been created between particles i and j by the aggregation model (see figure 2). (Here, we have used $m = 1$ and $k = 1$.)

3.2. The numerical method

We use the spectral moments method (SMM) [7, 8] which is a powerful tool for studying the dynamic properties of harmonic systems. This method has been applied to the study of fractal structures, percolation networks and silica aerogels [9, 10]. To compute the spectral dimension, we apply an extension of the SMM. The DOS is given by

$$g(\omega) = \sum_j \delta(\omega - \omega_j) \tag{6}$$

where ω_j is the frequency of the jth eigenmode, the eigenvalue λ_j of the dynamic matrix $\mathcal{D}$ being equal to the square of the frequency. It is more convenient to work with $u = \omega^2$ and $\lambda_j = \omega_j^2$, and compute

$$G(u) = \sum_j \delta(u - \lambda_j) \tag{7}$$

which is the squared frequency distribution. It is well known that

$$g(\omega) = 2\omega G(\omega^2). \tag{8}$$

$G(u)$ can be written as

$$G(u) = -\frac{1}{\pi} \lim_{\varepsilon \to 0^+} \{\mathrm{Im}\,[R(z)]\} \tag{9}$$

where $z = u + \mathrm{i}\varepsilon$, and $R(z)$ is the Stieljes transform of $G(u)$. One can show that [7]

$$R(z) = \mathrm{Tr}((zI - \mathcal{D})^{-1}) = \frac{1}{AM} \sum_\alpha (q^\alpha, (zI - \mathcal{D})^{-1} q^\alpha) \tag{10}$$

where (x, y) is the usual scalar product between vectors x and y. Then $G(u)$ can be deduced from $R(z)$. M is the number of q^α-vectors whose components are randomly taken between -0.5 and $+0.5$ ($\alpha = 1, \ldots, M$). Accurate results are obtained if $MN \propto 10^6$. With $N \propto 10^3$, it is necessary to average the DOS over about $M = 200$ systems. In the following, there is a double average: one on the structures of the aggregates, for a given

value of D, and another for a given system with M different values of the q^α-vectors. Now, the method consists in developing $R(z)$ in a continued fraction

$$R^\alpha(z) = \cfrac{b_0^\alpha}{z - a_1^\alpha - (b_1^\alpha/\{z - a_2^\alpha - [b_2^\alpha/(z - a_3^\alpha - \ldots)]\})} \tag{11}$$

for a given system and each value of the q^α-vectors. The coefficients a_n^α and b_n^α are calculated from the dynamic matrix. The generalized moments of $G(u)$ can be written as

$$\nu_n^\alpha = \langle q^\alpha | Q_n^\alpha(\mathcal{D}) Q_n^\alpha(\mathcal{D}) | q^\alpha \rangle \tag{12}$$

$$\overline{\nu_n^\alpha} = \langle q^\alpha | Q_n^\alpha(\mathcal{D}) \mathcal{D} Q_n^\alpha(\mathcal{D}) | q^\alpha \rangle \tag{13}$$

with

$$Q_{n+1}^\alpha(\mathcal{D}) = (\mathcal{D} - a_{n+1}^\alpha) Q_n^\alpha(\mathcal{D}) - b_n^\alpha Q_{n-1}^\alpha(\mathcal{D}) \tag{14}$$

and with the initial conditions $Q_{-1}^\alpha = 0$ and $Q_0^\alpha = 1$. We obtain

$$a_{n+1}^\alpha = \frac{\overline{\nu_n^\alpha}}{\nu_n^\alpha} \tag{15}$$

$$b_n^\alpha = \frac{\nu_n^\alpha}{\nu_{n-1}^\alpha}. \tag{16}$$

Relations (15) and (16) allow the determination of $R(z)$ and, thus, $g(\omega)$. In practice, the method consists in starting with q^α, computing ν_0 and $\overline{\nu_0}$ from (12) and (13), then computing a_1 and b_1, and so on. The method can be summarized by the following scheme, with $b_0 = 1$

$$|q^\alpha\rangle \longmapsto \left\{ \begin{array}{ll} \nu_0 & = \langle q^\alpha | q^\alpha \rangle \\ \overline{\nu_0} & = \langle q^\alpha | \mathcal{D} | q^\alpha \rangle \end{array} \right\} \longmapsto a_1^\alpha,\ Q_1^\alpha(\mathcal{D}) \longmapsto a_2^\alpha, b_1^\alpha \ldots \tag{17}$$

and

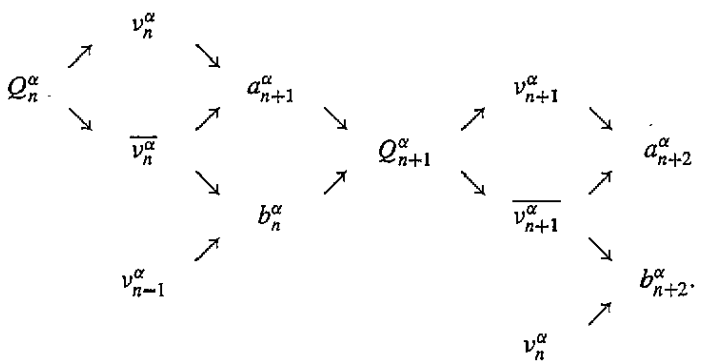

(18)

The SMM gives very good results with very large systems. If the system is smaller ($N \propto 10^3$), some difficulties appear when computing the slope of the log–log plot of the density of states. We find fluctuations which arise from the presence of small gaps in the spectrum. Then, the computed slopes are largely dependent on the value of the parameter ϵ. Such an effect does not appear when computing with very large systems. In order to obtain very accurate results, we have directly computed the integrated density of states (IDOS). We compute the function $H(u)$, such that

$$H(u) = \int_0^u G(u')\,\mathrm{d}u' \tag{19}$$

so from (19)

$$H(u) \propto u^{d_s/2}. \tag{20}$$

From equation (10), one obtains

$$R(z) = \frac{1}{AM} \sum_{\alpha} \sum_{j} \frac{|a_j^\alpha|^2}{z - \lambda_j} \tag{21}$$

with

$$a_j^\alpha = \sum_n q_n^\alpha \langle n|j\rangle \tag{22}$$

where $\langle n|j\rangle$ is the nth component of the eigenvector $|j\rangle$ and where q_n^α is the nth component of the q^α-vector defined above. Let us define $F(u)$, such that

$$F(u) = \oint_C R(z)\,\mathrm{d}z \tag{23}$$

where the contour C is a circle $R = u$. From (21), (23) and Cauchy theorem, one obtains

$$F(u) = \frac{2\pi \mathrm{i}}{AM} \sum_{\alpha} \sum_{j \in \lambda_j < u} |a_j^\alpha|^2 = \frac{2\pi \mathrm{i}}{AM} \sum_{\alpha} \sum_{\lambda_j < u} \sum_{n,n'} q_n^\alpha q_{n'}^\alpha \langle n|j\rangle \langle j|n'\rangle \tag{24}$$

where q_n^α are random numbers such that [7]

$$\frac{1}{M} \sum_{\alpha} q_n^\alpha q_{n'}^\alpha = A\,\delta_{n,n'}. \tag{25}$$

So, we have found that

$$F(u) = 2\pi \mathrm{i} \sum_{j \in \lambda_j < u} \left(\sum_n \langle n|j\rangle \langle j|n\rangle \right) \tag{26}$$

and, using the orthogonality of eigenvectors, one finds that

$$F(u) = 2\pi \mathrm{i} H(u) \tag{27}$$

which allows us to compute the integrated density of states directly from the generalized moments. In practice, we cut the integration on the complex domain into two parts

(i) positive angle, with $+\delta < \theta \leqslant +\pi$;
(ii) negative angle, with $\pi < \theta < -\delta$.

The radius u of integration is very finely discretized from 0 to u_{max}. To improve the efficiency of results found with the SMM, we present, in figures 3(*a*) and (*b*), graphs of $\log(H(u))$ versus $\log(u)$ for small systems, compared with results obtained by direct diagonalization (which gives exact results). As the computation of diagonalization is limited to matrices no larger than about 2000×2000, we have used SMM on aggregates of 2048 particles, to give a good comparison. For the other calculations, we have worked on samples with 8192 particles. In figure 3, we have averaged all the simulations on five samples of 2048 particles for the two methods (open triangles for SMM and solid line for diagonalization).

4. Brownian diffusion on a fractal aggregate

An alternative way to determine the spectral dimension is to study random walks on the same fractal aggregates.

The fundamental property of the random walks in which we are interested is the variation of the mean square displacement from the origin at time t (t being here the number of steps

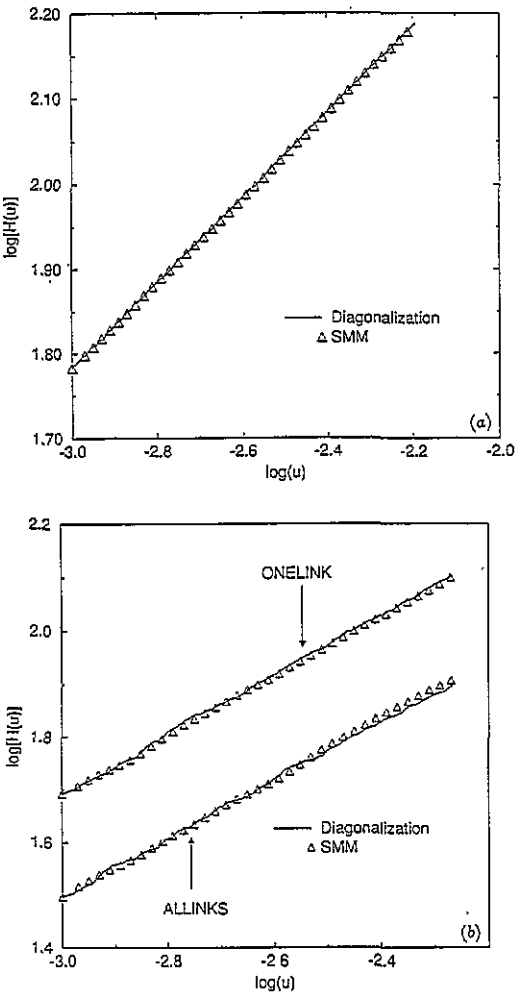

Figure 3. A comparison between the moments and diagonalization methods for aggregates of 2048 particles, averaged over five samples. A plot of $\log(H(u))$ versus $\log(u)$ in the case of: (*a*) a linear chain; (*b*) fractal aggregates of dimension $D = 1.60$, ALLINKS and ONELINK cases (open triangle for SMM, solid line for diagonalization).

performed on the aggregate). An exponent ν is introduced to describe the asymptotic behaviour [3]

$$\langle R^2(t)\rangle \propto t^{2\nu} \tag{28}$$

for large t.

With scaling arguments, it is shown that, on a fractal structure [3]

$$\nu = \frac{d_s}{2D} \tag{29}$$

where d_s is the spectral dimension and D the fractal dimension. In a Euclidean space of dimension d, it is well known that $\nu = \frac{1}{2}$. As it should be, the standard value $\frac{1}{2}$ is recovered on a Euclidean lattice, where $d_s = D$. With (29), relation (28) becomes

$$\langle R^2(t)\rangle \propto t^{\frac{d_s}{D}} \qquad t \to \infty. \tag{30}$$

In accordance with (30), we have performed random walks on aggregates of $N = 2048$ particles, for 1000 steps, averaged over 100 different starting sites. Each starting particle is chosen randomly in a small cubic box, containing the centre of mass of the aggregate. We have also averaged over five different samples in order to minimize fluctuations. Figure 4 presents three examples of plots obtained with the diffusion method: a log–log plot of $\langle R^2(t)\rangle$ versus t for a linear chain (a) and for aggregates with fractal dimension $D = 2.18$, in the two cases ONELINK and ALLINKS (b).

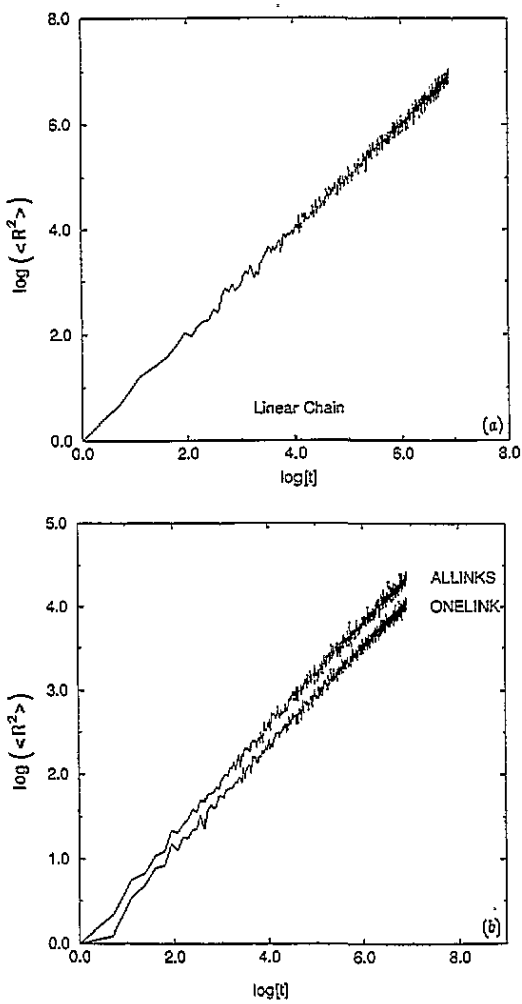

Figure 4. A plot of $\log\langle R^2(t)\rangle$ versus $\log(t)$ (where t is the number of steps), in the case of: (a) a linear chain ($d_s = 1$); (b) fractal aggregates of dimension $D = 2.18$, in the ALLINKS ($d_s = 1.345$) and ONELINK ($d_s = 1.288$) cases.

5. Results and discussion

First, let us consider the SMM results, reported in figure 5. In the two cases, the value of d_s increases monotically with D, and, for large values of D, the results for d_s are larger

for the ALLINKS than for the ONELINK model. In both the ALLINKS and ONELINK models, the results for $D \lesssim 2$ are almost superimposed and well fitted (within the error bars) by the linear relationship $d_s \simeq 1 + 0.2(D-1)$. For $D \gtrsim 2$, they separate: while d_s becomes almost independent of D ($d_s \simeq 1.20$) in the ONELINK case, it increases more rapidly in the ALLINKS case (but we have not got enough data to provide a reliable fit). This last result can be understood since d_s should tend to three in the ALLINKS case when $D \to 3$, while there is no obvious $D = 3$ limit in the ONELINK case.

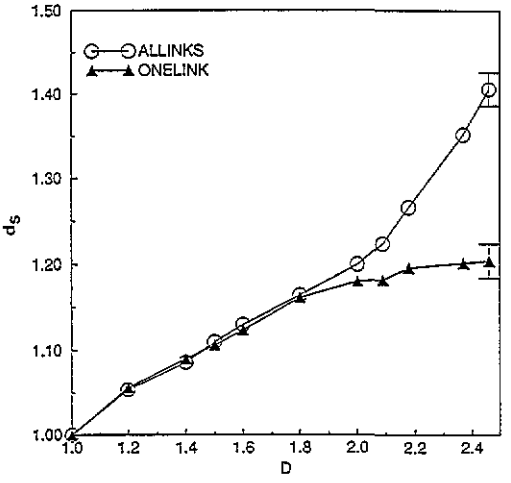

Figure 5. The spectral dimension calculated by the moments method, for aggregates with 8192 particles, averaged on five samples. We present the two cases: ALLINKS and ONELINK.

Let us now present the results of the Brownian diffusion method (figure 6). The same qualitative behaviour is observed but the curves separate earlier, at about $D \simeq 1.8$. Here the differences between the ALLINKS and ONELINK cases for large D-values are explained by the large probability of the random walk returning to the origin due to the existence of loops in the ALLINKS case. In principle, there should be no difference between the two methods and we think the discrepancies between figure 5 and figure 6 might be explained by systematic finite-size errors. This is illustrated in figure 7, where we have plotted d_s versus $1/N$ for two typical values of D (below and above $D \simeq 2$) in the two ALLINKS (a) and ONELINK (b) cases (diffusion is represented by circles and SMM by triangles, with filled symbols for $D = 2.20$ and open symbols for $D = 1.50$). For large systems, the results of the SMM method are nearly independent of size whilst the random-walk results depend on size, more significantly for $D = 2.2$ than for $D = 1.50$, and support the conjecture of the same asymptotic ($N \to \infty$) limit as found with the SMM. Therefore the differences between the random-walk method and the SMM for $D > 2$ are certainly purely artifactual and arise from the strong finite-size errors in the random-walk case.

Furthermore, let us show how the SMM method can be compared with a third estimate of d_s based on the Alexander and Orbach formula [3]

$$\omega_c^2 \propto N^{-2/d_s} \tag{31}$$

where ω_c is the phonon–fracton crossover frequency. In our model, there are no phonon modes. So, ω_c is the lowest non-zero frequency of the spectrum [3]. We have plotted $\log(\omega_c^2)$ versus $\log(N)$ (an example for $D = 1.5$ is shown in figure 8) and found very good

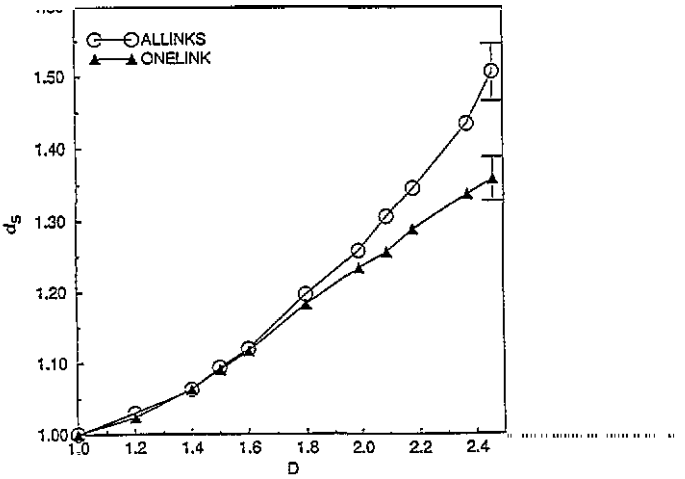

Figure 6. The spectral dimension calculated by the diffusion method, for aggregates with 8192 particles, averaged over five samples. We present the two cases: ALLINKS and ONELINK.

results—in both ALLINKS and ONELINK cases. We summarize the results for d_s, for $D = 2.20$ and $D = 1.50$, in table 1.

Table 1. A comparison of results obtained for d_s with the spectral moments method (SMM) and using the Alexander and Orbach formula (AOF) for two significant values of D.

	$D = 1.50$	d_s	$D = 2.20$	d_s
ONELINK	SMM	1.13	SMM	1.184
	AOF	1.111	AOF	1.197
ALLINKS	SMM	1.100	SMM	1.250
	AOF	1.104	AOF	1.246

6. Comparison with experiments and conclusion

In this paper, we have obtained an explicit variation of the spectral dimension d_s as a function of the fractal dimension for a series of aggregates of tunable fractal dimension and we have shown that including loops can subsequently increase d_s, at least for large fractal dimension. At this stage it might be tempting to compare the present theoretical results with the existing experiments, especially in the case of aerogels, where the existence of fractons has been best demonstrated. The spectral dimension of aerogels has been estimated by Brillouin scattering experiments giving $d_s \simeq 1.1$ in the case where they are prepared with a basic catalyser [11] and $d_s \simeq 1.3$ without a catalyser [12]. The spectral dimension of basic aerogels is in remarkably good agreement with the present work if one knows that their fractal dimension is $D = 1.8$ [13], a value corresponding to $d_s \simeq 1.15$ in both the ONELINK and ALLINKS cases. Moreover, it is known that small-angle neutron scattering experiments are very well accounted for by numerical simulations based on the diffusion-limited cluster–cluster aggregation model [14] which is a model very close to the variable-D model for $D = 1.8$. To discuss the case of neutral aerogels, one should consider that a fractal dimension of $D = 2.3$ gives here $d_s \simeq 1.2$ in the ONELINK case and $d_s \simeq 1.3$

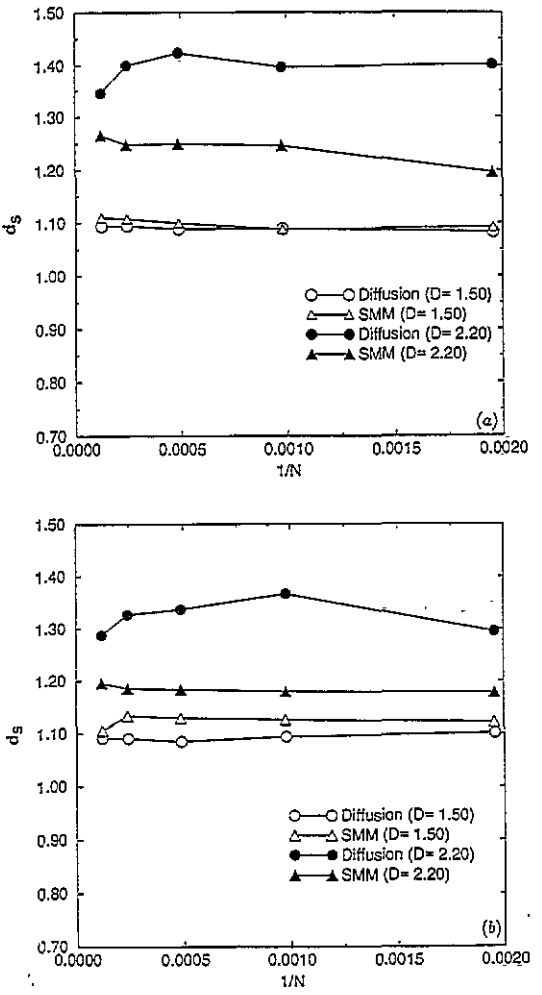

Figure 7. Fluctuations due to size effects and aggregate structures for $D = 1.50$ (open symbols) and 2.20 (filled symbols), for $N = 512$, 1024, 2048, 4096 and 8192 particles, for (a) the ALLINKS case; (b) the ONELINK case. (Diffusion method (circle), SMM (triangle).)

in the ALLINKS case. Again, this seems to be in good agreement with the experiments if one knows that the structure of neutral aerogels is of a polymeric nature and certainly has many more loops than the structure of basic aerogels. However, there has been a recent interpretation of the neutral aerogel experimental results concluding that there is a smaller ($D \simeq 2$) fractal dimension [15]. In this framework, it would be necessary to include many more loops and/or much more connectivity, to explain the relatively high value of d_s. Unfortunately, this is outside the scope of the present modelling. Overall, it is important to notice that here we have used a scalar model, while in experiments the tensorial nature of the vibrations has been evident, as some torsion modes have been invoked, even in the case of basic aerogels [11]. Therefore it is our intention to extend the present calculations to the case of more complicated potentials, taking care of the tensorial character of the vibrations in order to test whether the d_s-values are modified or not. This is a more difficult task and, to our knowledge, such a study has only been done on percolation clusters up to now [4].

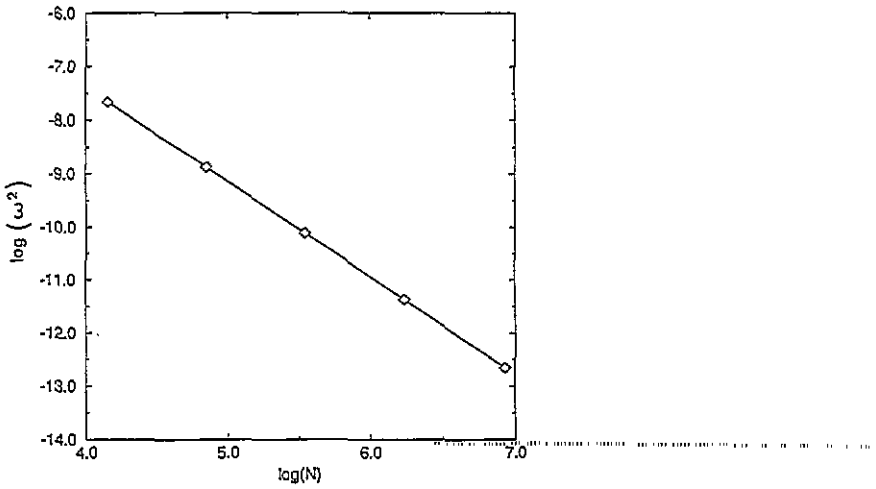

Figure 8. A plot of $\log(\omega_c^2)$ versus $\log(N)$, in the ONELINK case, for $D = 1.50$. With formula (31) we obtain $d_s = 1.11$ ($d_s = 1.106$ with SMM).

We think that using the variable-D model would be a great improvement and would clarify comparisons with experimental results.

Acknowledgments

We would like to thank E Anglaret for interesting discussions and G Urbach for his technical help in parallel computing. Numerical calculations were done with the help of the computers of the CNUSC (Centre National Universitaire Sud de Calcul).

References

[1] Jullien R and Botet R 1987 *Aggregation and Fractal Aggregates* (Singapore: World Scientific)
[2] Thouy R and Jullien R 1994 *J. Phys. A: Math. Gen.* **9** 2953
[3] Alexander S and Orbach R 1982 *J. Phys. Lett.* **43** L625
[4] Nakayama T, Yakubo K and Orbach R L 1994 *Rev. Mod. Phys.* **66** 381
[5] Ball R and Jullien R 1984 *J. Physique Lett.* **45** L1031
[6] Warren P B 1993 *J. Physique* I **XX** 1509
[7] Benoit C, Royer E and Poussigue G 1992 *Phys. Condens. Matter* **4** 3125
[8] Benoit C 1994 *J. Phys.: Condens. Matter* **6** 3137
[9] Rahmani A, Benoit C and Royer-Vilanova E 1993 *J. Phys.: Condens. Matter* **5** 7941
[10] Rahmani A, Benoit C and Poussigue G 1994 *J. Phys.: Condens. Matter* **6** 1483
[11] Anglaret E, Hasmy A, Courtens E, Pelous J and Vacher R 1994 *Europhys. Lett.* **28** 591
[12] Courtens E, Vacher R, Pelous J and Woignier T 1988 *Europhys. Lett.* **6** 245
[13] Vacher R, Woignier T, Phalippou J, Pelous J and Courtens E 1988 *J. Non-Cryst. Solids* **106** 161
[14] Hasmy A, Anglaret E, Foret M, Pelous J and Jullien R 1994 *Phys. Rev.* B **50** 6006
[15] Jullien R and Hasmy A 1995 *Phys. Rev. Lett.* **74** 4003